Journal of Materials Science & Surface Engineering, 6(2): 761-766
ISSN (Online): 2348-8956; 10.jmsse/2348-8956/6-2.1

Gelatin-Silk Fibroin Composite Scaffold as A Potential Skin Graft Material

Preethi Ramadoss[1] . V. Subha[2] . S. Kirubanandan[2]

[1]Crystal Growth Centre, Anna University, Chennai-25, India.
[2]Centre for Biotechnology, Anna University, Chennai-25, India.

ABSTRACT
The study presents a detailed comparison of the morphological, mechanical and biological differences that takes place upon the addition of silk fibroin to gelatin biomaterial. 3D porous scaffolds of pure gelatin (G) and gelatin, silk (GS) composite were fabricated by freeze drying. The incorporation of silk fibroin into the gelatin scaffold has provided a remarkable flexibility to the scaffold. Biomimetic composite was fabricated with gelatin and silk and this scaffold can be used as a skin graft material. The scaffolds were also tested for their electrical admittance and it was found that the addition of silk has given a better electrical admittance. Therefore, this will help in wound healing treatments that require electrical stimulations. Together with all the biological, physico-chemical, morphological, thermal and mechanical properties, Gelatin -Silk composite is an excellent biocompatible material that can be used for fabricating scaffolds for skin regeneration/skin tissue engineering applications.

ARTICLE HISTORY
Received 06-11-2017
Revised 05-01-2018
Accepted 08-01-2018
Published 02-04-2018

KEYWORDS
Silk fibroin,
Gelatin,
Tensile property,
Skin graft material,
Physio-chemical-characterization

Introduction

The injured skin requires replacement that demands an autograft which is another part of skin from the same individual that is used to replace the damaged area of the injured skin. However, this clinical trial involves two surgeries on the same individual causing discomfort. Therefore, the bioengineered skin substitutes are being used to replace any damaged part of the human skin. A bioactive scaffold fabricated to be implanted onto an injury site should provide support for the cells to grow. The scaffold should be bioactive and provide a platform for cellular microenvironment for cell fate processes. To achieve the objective of tissue reconstruction capability of scaffold, it should satisfy the specific prerequisite such as biocompatibility, pore size and good porosity. High porosity and a sufficient size of pores in the scaffold are required mandatorily for seeding the cells and good diffusion of bioactive molecules through tissue structure. Silk Fibroin is a protein based natural polymer that has been used in textiles for centuries. More recently, it has been used as a starting material for medical and tissue engineering scaffold applications due to its high tensile strength and biocompatibility. In nature, silk is coated with sericin, which must be removed to purify silk fibroin. Sericin acts like glue which helps to maintain the structure of the cocoon [1]. However, in terms of using silk as a biomaterial, sericin can cause an adverse immune response if implanted [2]. The gummy sericin is easily removed by boiling the cocoons in aqueous sodium carbonate [3]. The fiber consists of two cores of fibroin covered with a layer of sericin [1]. Silk fibroin consists of a heavy and light chain (350 kDa and 25 kDa), that are linked by a disulfide bond. Overall, silk fibroin is a negatively charged protein at a neutral pH and has an isoelectric pH of approximately 3.8 [4]. Hydrophobic interactions cause the protein's random coil formation to change to a β-sheet formation, which is the reason behind silk's exceptional tensile strength [5]. Gelatin was chosen in this study because it is a denatured form of collagen that is the major component of skin, bones and connective tissues. The purified gelatin does not show signs of antigenicity, thus it is one of the most suitable proteins to be used in tissue engineering and is less expensive than collagen [6, 7]. Gelatin shows interesting biological characteristics since it contains arginine-glycine-aspartic acid (RGD) like sequence which promotes cell attachment and proliferation, thus making it suitable for tissue engineering applications [8]. This work reports on gelatin/silk (GS) prepared by freeze- drying technique for physicochemical, mechanical and hemo-compatible were carried out.

Experimental

Extraction of Silk Fibroin

Unpolished Bombyx Mori Silk was obtained and degummed by boiling the silk in 0.02M Na_2CO_3 and rinsed thoroughly with distilled water and dried. It is then dissolved in 200 ml of a solution containing a mixture of $CaCl_2$: H_2O: Ethanol in the ratio of 1:8:2 respectively at 60°C for approx 12 hrs. The resultant salt/silk solution is then dialyzed against water with a cellulose membrane for a week. 150 ml of Silk Fibroin solution was obtained from 5g of silk It was then centrifuged for 40 mins at 9000 rpm to remove the impurities.

Quantification of the extracted proteins

The quantity of protein in the extracted solutions was determined by the dry weight method. Where, 1 ml of protein solution is weighed and dried in vacuum oven at 60°C for 8 hours. The obtained weight difference between the protein before and after drying was taken as the final concentration of the protein. The concentration of obtaining silk fibroin after thorough dialysis is 15 mg/ml.

Preparation of the scaffolds

Two scaffolds were prepared viz G and GS. 12% Gelatin (Sigma Aldrich) was dissolved in deionised water to

Corresponding Author: S. Kirubanandan, Tel: +91956620460
Email: skirubanandan80@gmail.com

Contents lists available at http://www.jmsse.in/ & http://www.jmsse.org/

prepare G, whereas, 3.6 g of Gelatin was mixed with 30 ml of 12% (w/w) silk fibroin by stirring it at 60°C for 6 hrs in order to fabricate GS. The obtained mixture was allowed to cool at 25°C followed by pre-freezing at -25°C for 24hrs before lyophilising the composites at-110°C. The freeze-dried scaffolds were subsequently crosslinked with 0.4% glutaraldehyde at room temperature for 2 hours and then washed and lyophilized once again.

Characterization of Scaffolds

Scanning electron microscope (SEM) (Carl Zeiss MA 15/EVO 18) was used to observe the surface morphology of the scaffolds. The samples were coated with gold and palladium alloy coating of about 5-10 nm thickness with the help of Sputter coater (Quorum SC 7620) prior to investigation. FTIR (Fourier Transform Infrared Spectrometer) analysis was carried out with the help of Jasco International Co. /Japan Fourier Transform Infrared Spectrometer Model FTIR-6300 in ATR mode. The particle size and zeta potential of the proteins were measured with the help of DLS (Dynamic Light Scattering), ZEN 3600 He-Ne laser (633 nm) at a refractive index of 1.54. Tensile strength was analyzed with the help of Instron 3369 with a load cell of 100 N. The samples with 4cm X 1cm dimensions were soaked in saline solution prior to testing. The samples were loaded in the tester and loads of different magnitudes (0-1N) were applied at gradual increment. Contact angle measurement was performed with the help of USB Microscope. The samples were placed on a flat surface on top of which a drop of deionized water was placed and the picture was captured. The angle of the water droplet is measured with the help of ImageJ software. The DSC analysis was carried out using SII Nanotechnology DSC 6220 in the temperature range of 30-350 °C.

Results and Discussion

FTIR

The Fourier Transform Infrared (FTIR) spectrum of the samples as shown in Figure 1. The characteristic peaks at 1631 cm^{-1} (amide I, C=O bond), 1536 cm^{-1} (amide II bending of N–H bond) and 1455cm^{-1} (stretching of C–N bond in amide III) confirms the presence of gelatin. The absorption peaks (GS) at 1624 cm^{-1}, 1536 cm^{-1}, 1222 cm^{-1} correspond to amide I, amide II and amide III respectively. The peaks at 1624 cm^{-1} and 1536 cm^{-1} represents the β Sheet Confirmation of amide I and the random coil for Amide II respectively. The band at 1222 cm^{-1} corresponds to the random coil of Amide III. It has already been reported that the amide I of silk fibroin is associated with the α-helical conformations are represented by bands between 1650 cm^{-1} and 1660 cm^{-1}, whereas the random coil conformations are represented by bands between 1640 cm^{-1} and 1650 cm^{-1}. The β-sheet conformations are represented by bands between 1620 cm^{-1} and 1640 cm^{-1}.

SEM

Scanning electron microscopic (SEM) images were taken for the silk before and after degumming to make sure that sericin are removed completely. The white sediments like particles present in Figure 2(a) is the sericin content which seem to be absent after degumming as shown in Figure 2(b).

SEM micrographs of the composites show that the addition of silk fibroin to gelatin, has led to the formation of an interconnected porous structure as opposed to the pure gelatin scaffolds. Plain Gelatin scaffold showed an average pore size of approximately 11±2 µm (Figure 2), whereas the pore size increases to around 13±11 µm in Gelatin Silk (GS) composite. Highly porous scaffolds will provide sufficient space for cell growth; it will also facilitate waste exchange for the growth of healthy cells and extracellular matrix production [10]. Further, the addition of gelatin not only involved the structural transformation of silk fibroin but also facilitated the interactions between silk fibroin and water, which ensued the formation of porous structure. The average sizes of the human cells lie within the range of 2-120 µm [11]. Hence, from the SEM micrographs it is clear that the fabricated G and GS scaffolds can accommodate all kinds of cells and facilitate free movement of cells within the matrix. Figure 3 shows the fibers of silk before and after degumming .

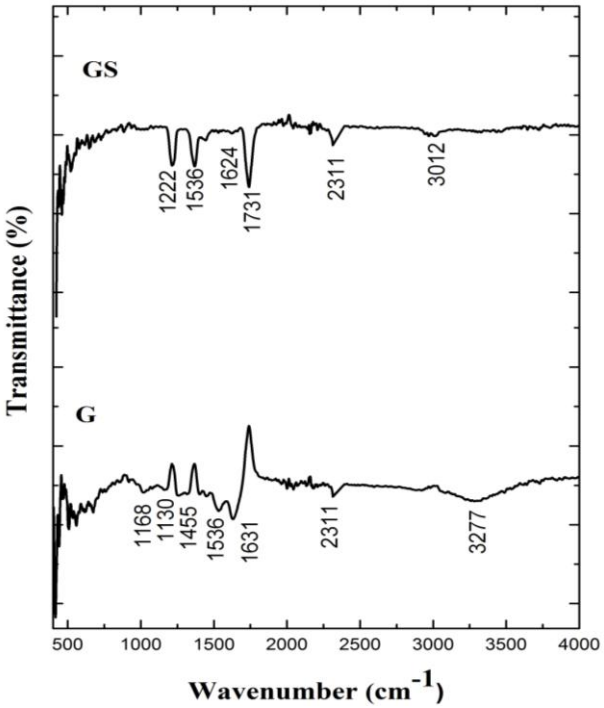

Figure 1: FTIR spectra of Pure Gelatin (G) and GS

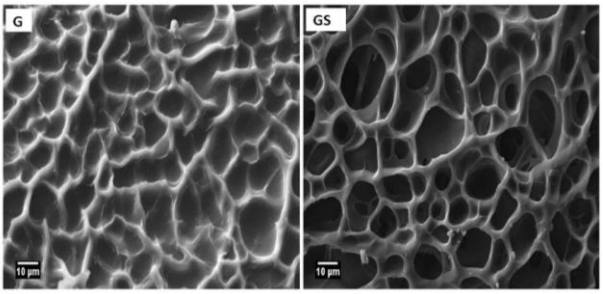

Figure 2: SEM images of G and GS scaffolds

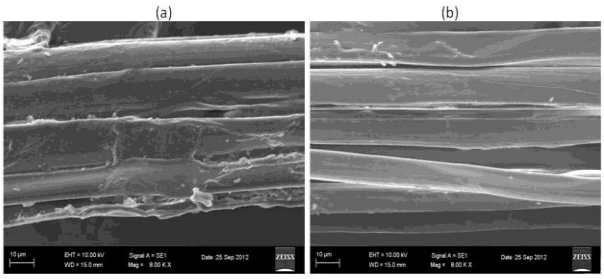

Figure 3: SEM images of Silk fibers (a) before and (b) after degumming

Particle Size

The respective particle size of the extracted silk fibroin protein and gelatin (12%) as measured by DLS was 0.660 µm and 33 µm (Table 1). The particle size of the proteins plays a vital role in the formation of pores in the scaffold as confirmed by SEM images that show porous structures upon the addition of silk. The enhancement of the average pore size and distribution in GS can be explained as follows. The gelatin particles have the tendency to agglomerate at higher concentrations and in this case the concentration being 12% the pores are shallow and non-homogenous (Figure 4). Upon addition of silk fibroin to the colloidal gelatin solution, the gelatin interacts with silk particles, thus separating the gelatin particles from each other, thereby showing interconnected, larger and evenly distributed pores (Figure 5).

Table 1: The particle Size of Gelatin and Silk Fibroin

Proteins	Particle Size
Gelatin	33 µm
Silk	0.66 µm

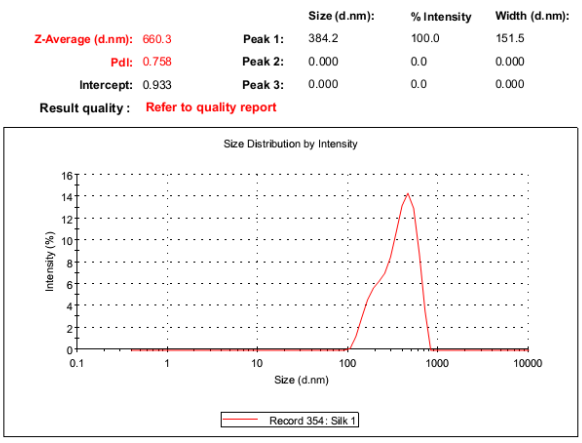

Figure 4: Size Distribution of Gelatin Particle

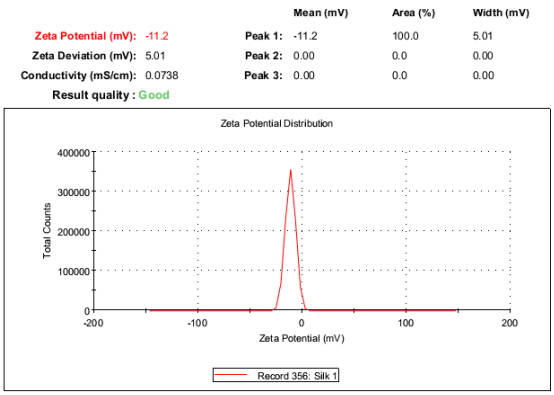

Figure 5: Size Distribution of Silk Particle

Zeta Potential

The surface of the gelatin (-17 mv) and silk fibroin (-11 mv) particles are found to be negatively charged (Table 2). It is generally preferred that the surface charge of the material to be implanted is positively charged as the cells in the human body have a negatively charged cellular membrane [12]. Although this material is negatively charged, cellular uptake can be doubled after implantation by creating a voltage potential across the implanted site to facilitate a quicker wound healing process.

Table 2: The Zeta Potential of Gelatin and Silk

Proteins	Zeta Potential
Gelatin	-17 mV
Silk	-11 mV

Voltage Admittance

Individual cells maintain an electrical voltage across the plasma membrane (Vm) as a consequence of the action of membrane-bound ion channels. The electrical potential at the epidermis is known as "transepithelial potential" (TEP) and varies between 10 mV and 60 mV (average, 23 mV) [13]. During injuries, this epithelial seal is broken and the TEP drastically reduces at the wound site and the ions immediately begin to leak out. As wounds require different types of cells at various stages of healing, these cells have different polarization. The application of electrical simulation decreased the wound related pain and increased the cutaneous blood flow [13]. Bassett & Hermann have proved that the DNA and collagen synthesis in fibroblasts can increase up to 160% after 14 days of treatment, when the cathode potential is between 50 and 75V and 100 PPS (pulses per second), leading to the efficient healing of the wound. The cathode attracts anions (negatively charged ions) while the anode attracts cations (positively charged ions). Cells attracted to the cathode include neutrophils fibroblasts, and epidermal cells [15, 16]. The effects of using the cathode include re-epithealization and a non-painful, selective removal of nonviable tissue called autolytic debridement [14]. Macrophages are an example of cells attracted to the anode [17]. The anode can promote the formation of granulation tissue and decrease inflammation and infection within the wound bed [18]. High Volt Pulsed Current (HVPC) is the most commonly used modes of electrical stimulation for wound care, however, some research indicates the use of Direct Current (DC) for antiseptic effects [19].

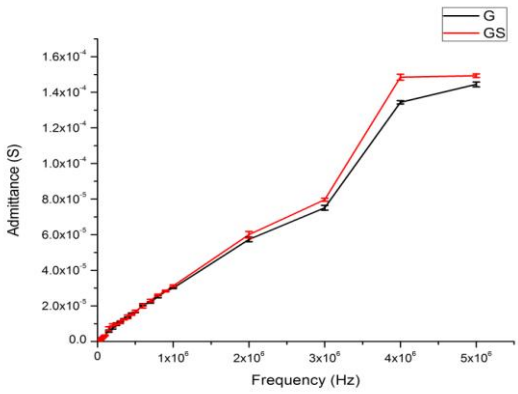

Figure 6: Voltage admittance of G and GS

The electrical properties of the composites were studied and their potential of conducting electricity was compared

and it is found that both the scaffolds conduct electricity in the range 1.2-1.5 x 10^{-4} S for the frequency range 50-5 x 10^{6} Hz., confirming that the scaffolds could conduct electricity thereby enabling a quicker wound healing process (Figure 6).

Differential Scanning Calorimetry (DSC)

The DSC thermographs (Figure 7) of the composites revealed that the GS has higher thermal stability when compared to G. Endothermic peaks start at 75 °C and 82 °C in G and GS respectively, and their corresponding melting/degradation peak is 216 °C and 231 °C respectively. The addition of silk fibroin has increased the Tg (glass transition temperature) to 231 °C. The endothermic peaks observed in the range of 200-350°C can be assigned to the protein denaturation followed by protein degradation [20]. The Tg offers information about the stability of the non-crystalline parts in polymers. Thus, the increase of Tg confirmed that the interaction between gelatin and silk fibroin has changed the conformation composition of silk fibroin that resulted in a more stable non-crystalline silk fibroin structure. [21].

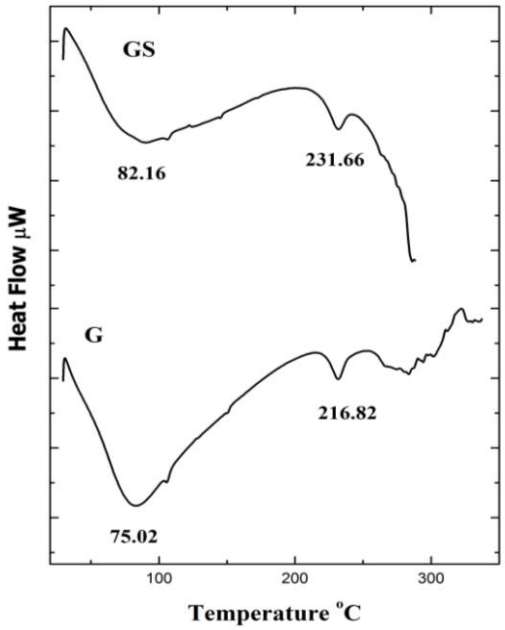

Figure 7: Thermogram of Gelatin and Gelatin Silk Scaffolds

Mechanical Strength

The mechanical property (Figure 8) of the scaffolds were evaluated by means of measurement of its tensile strain in wet condition, as these scaffolds are to be used as implants; hence these scaffolds were soaked in saline solution for 4 hrs before testing. To use the scaffold as a skin substitute, it has to be strong enough to support extensive vasculature, the lymphatic system, nerve bundles and other structures in the skin. Thus, the scaffold must have appropriate mechanical properties to absorb forces when they are embedded in the lesions. The tensile strain of G and GS were compared and it was found that GS had a much greater tensile strain (%) when compared to G, which could be due to the presence of the high content of hydrophilic amino acids when compared to that of pure gelatin. The elasticity of the material increases with an increase in the hydrophobicity [22].

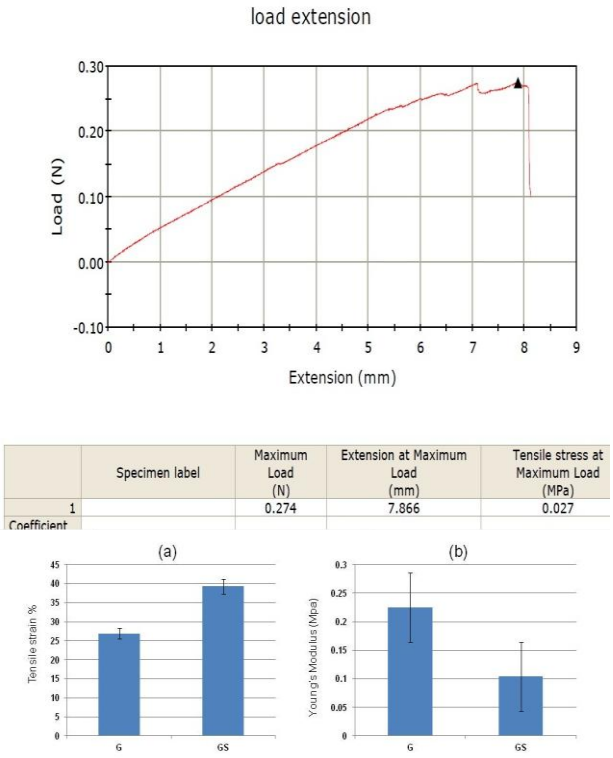

Figure 8: Mechanical Strength of G and GS (a) Tensile Strain (b) Young's Modulus

Contact Angle

The contact angle was measured for the two scaffolds and was found that GS (53±1°) had a lower contact angle when compared to G (57±1°) (Figure 9). The addition of silk fibroin has made the scaffold, hydrophilic when compared to pure gelatin scaffold.

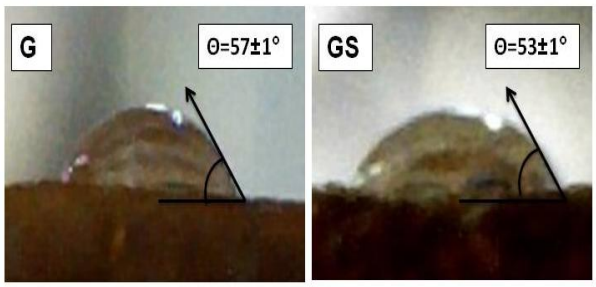

Figure 9: Contact Angle measurements of G and GS

Molecular Docking of Silk and Gelatin

Hydration is very important for the three-dimensional structure and activity of proteins. Hydrogen bonding adds conformational flexibility, while the level of hydration determines the degree of flexibility in the internal molecular motions [23]. Hydrogen bonding confers rigidity to the protein structure and specificity to intermolecular interactions. Non-bonded interactions are nothing but the electrostatic and hydrophobic interaction between the two proteins. There are three types of non-bonded interactions, which are electrostatic interaction, the van der Waals forces and hydrophobic interactions, of which the ion-ion (electrostatic) interaction is stronger than the dipole-dipole (vaan der Waals) interaction. The bonds that are formed between gelatin and silk (Figure 10), (Table 3) constitutes a mechanically stable structure. The tensile

strain of GS (40%) is more when compared to that of G (27%), which is due to the number of electrostatic interactions and hydrogen bonds, which gives the composite its flexibility.

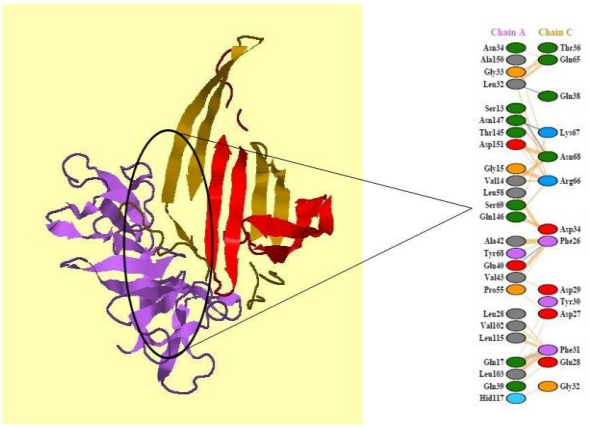

Figure 10: Molecular Docking of Gelatin and Silk

Table 3: No. of Bonds between Gelatin and Silk

GELATIN-SILK INTERACTION	
No. of Hydrogen Bonds	5
No. of Non-Bonded Contacts	255
No. of Amino Acids In Gelatin	160
No. of Amino Acids In Silk	268

Swelling ratio

The swelling behavior of the two scaffolds was studied and was found that GS has the maximum swelling ratio (467%) when compared to G which was 266% (Figure 11); this can be ascribed to the high proportion of hydrophilic amino acids present in it. Also, because gelatin is known to increase the interaction between silk and water [21], GS seems to have higher swelling behavior when compared to G.

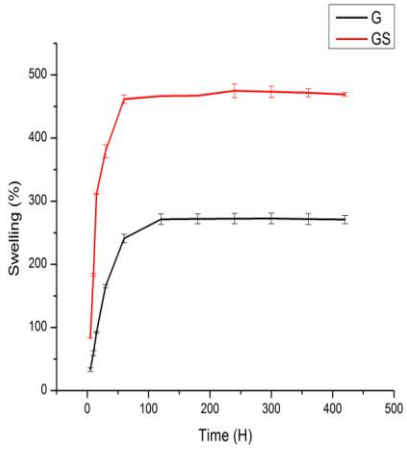

Figure 11: Swelling Percentage of G and GS

Hemolysis

Hemocompatibility was studied for the scaffolds to evaluate the disposition of that polymer composite to interact with our blood cells as they are to be engrafted into the skin and will eventually react with the blood cells beneath it (Figure 12). Therefore the quantity of blood cells that get lyzed upon implantation could be measured in vitro prior to implantation. Percentage of hemolysis is calculated utilizing the formula [24]. Hemolysis results of G and GS shows that the scaffolds exhibit minimum hemolysis lying well within the ASTM standards.

$$\% \text{ hemolysis} = \frac{\text{OD for the test sample} - \text{OD for the negative control}}{\text{OD for the positive control} - \text{OD for the negative control}}$$

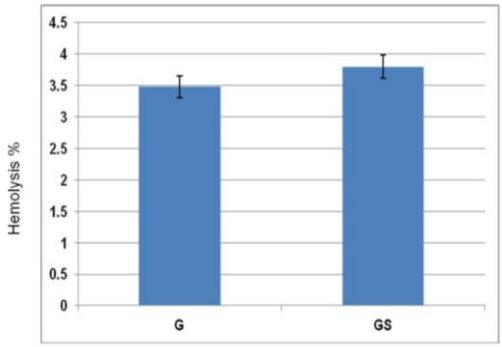

Figure 12: Hemolysis percentage of G and GS

Conclusions

The addition of silk fibroin protein to the gelatin scaffold has found to improve the functionality of the scaffold as much as a better implantable biomaterial when compared to the pure gelatin scaffold. The addition of silk has given the material a better and evenly distributed porosity when compared to pure gelatin scaffold in addition to it being hemocompatible. GS is more hydrophilic when compared to G which is proven by the swelling behavior of the two scaffolds. The contact angle measurements have also revealed that the hydrophilicity has increased upon addition of silk. The enhanced electrical admittance of the composite would facilitate the use of electrical simulation on the wound site, would promote better wound healing. The increase in hydrophilicity and intermolecular hydrogen bonding in GS has provided a better flexibility that can support neo tissue. The interaction between silk and gelatin has been found to be enhanced leading to an improved mechanical strength and stability. The addition of silk fibroin to gelatin has shown a remarkable increase in the elasticity which is the major requirement for skin graft. Therefore, the addition of silk to gelatin has made it potentially more suitable for skin replacement. The overall characteristics required for a good skin graft material has found to be satisfied by the incorporation of silk fibroin to gelatin. The material that was fabricated is completely natural and cost effective.

Acknowledgement

Preethi Ramadoss gratefully acknowledges Prof. S. Subramanian, Department of Textile Technology, Anna University, Chennai for providing the silk that was required for the research I would like to thank my friends Rohini Rangarajan, and Sumitra Menon for the scientific discussions.

References

1. Perez-Rigueiro J, Llorca MEJ & Viney C. Tensile Properties of Silkworm Silk Obtained by Forced Silking. Journal of Applied Polymer Sciences 2001; 82:1928-1935.
2. Haifeng Liu ZG, Yue Wang, Siew LT, Vallaya Sutthikkum & James CHG, Modification of sericin-free silk fibers for

ligament tissue engineering application. Journal of Biomedical Materials Research Part B: Applied Biomaterials. 2006; 10:129-138.
3. Zhengzhong Shao FV. Surprising strength of silkworm silk. Nature. 2002; 418: 741.
4. Shailesh Nagarkar TN, Christophe Chassenieux & Ashish Lele. Structure and gelation mechanism of silk hydrogels. Physical Chemistry Chemical Physics. 2010; 12: 3834-3844.
5. Qiang Zhang SY & Mingshong Li. Silk fibroin based porous materials. Materials 2009; 2: 2276-2295.
6. Buckley CT & O'Kelly KU. Regular scaffold fabrication techniques for investigations in tissue engineering', Topics in bio-mechanical engineering: proceedings of the 1st Symp. on Biomechanical Engineering, eds. P. J. Prendergast & P. E. McHugh, Dublin and Galway, Ireland. 2004. 147 –166.
7. Eisenbud D, Huang N, Luke S & Silberklang M. Skin substitutes and wound healing: current status and challenges. Wounds: A Compendium of Clinical Research and Practice. 2004;16(1):2-17.
8. Chamchongkaset J, Kanokpanont S, Kaplan DL & Damrongsakkul S. Modification of thai silk fibroin scaffolds by gelatin conjugation for tissue engineering. Advanced Materials Research. 2008; 55- 57: 685-688.
9. Kino R, Ikoma T, Yunoki S, Nagai N, Tanaka J, Asakura T & Munekata M. Preparation and characterization of multilayered hydroxyapatite /silk fibroin film, J. Biosci. Bioeng. 2007;103: 514–520.
10. Kang HW, Tabata T & Ikada Y. Biomaterials. 1999; 20: 1339–1344.
11. Arthur J Vander, James H Sherman & Dorothy S Luciano. Human Physiology: The Mechanisms of Body Function. 1990 Fifth Edition, McGraw-Hill Publishing Company, New York.
12. Rebl H, Finke B, Ihrke R, Rothe H, Rychly J, Schroeder K & Nebe B J. Positively Charged Material Surfaces Generated by Plasma Polymerized Allylamine Enhance Vinculin Mobility in Vital Human Osteoblastss, Adv. Eng. Mater. 2010; 12: B356–B364.
13. Bassett & Hermann. The effect of electrostatic fields on macromolecular synthesis in fibroblasts in vitro', J. Cell Biol. 1968; 39:9a.
14. Fukushima K, Senda N, Iuri H, Tamai Y & Mauakami U. Studies of galvanotaxis of leukocytes', Med. J. Osaka Univ. 1953; 4(2-3): 195-208.
15. Kloth L. Electrical Stimulation for Wound Healing: A Review of Evidence from In Vitro Studies, Animal Experiments, and Clinical Trials. International Journal of Lower Extremity Wounds, 2005; 4: 23-44.
16. Orida N & Feldman J. Directional protrusive pseudopodial activity and motility in macrophages induced by extracellular electric fields. Cell Motility. 1982;2: 243-255.
17. Shaw TJ & Martin P. Wound repair at a glance. Journal of Cell Science. 2009; 122: 3209–3213.
18. McCulloch JM & Kloth L. Wound healing: Evidence-based management, 4th edition. Philadelphia, Davis and Company, PA, F.A, 2010; 450-513.
19. Ong P, Laatsch L & Kloth L. Antibacterial effects of a silver electrode carrying microamperage direct current in vitro', Journal of Clinical Electrophysiology. 1994; 6(1):14-18.
20. Spei M & Holzem R. Helix content of extended and annealed keratins. In The 8th International Wool Textile Research Conference. 1990; 1: 488-497.
21. Qiang Lu, Xiaohui Zhang, Xiao Hu & Kaplan DL. Green Process to Prepare Silk Fibroin/Gelatin Biomaterial Scaffolds. Macromol. Biosci. 2010; 10(3):289-298.
22. Isabelle V & Lan T. Biodegradable Polymers. Materials. 2009; 2:307-344.
23. Hydrogen bond. Available from: <http://en.wikipedia.org/wiki/ Hydrogen bonding.
24. Chowdhury SKR, Mishra A, Pradhan B & Saha D. Wear characteristic and biocompatibility of some polymer composite acetabular cups. Wear. 2004; 256: 1026-1036.